Energy 239 (2022) 121914

Contents lists available at ScienceDirect

Energy

journal homepage: www.elsevier.com/locate/energy

Energy consumption modelling of a passive hybrid system for office buildings in different climates

Yi Zhang [a], Thilhara Tennakoon [a], Yin Hoi Chan [a], Ka Chung Chan [a], Sau Chung Fu [a], Chi Yan Tso [b], Kin Man Yu [c], Bao Ling Huang [d], Shu Huai Yao [d], Hui He Qiu [d], Christopher Y.H. Chao [a, *]

[a] *Department of Mechanical Engineering, The University of Hong Kong, Pokfulam, Hong Kong*
[b] *School of Energy and Environment, City University of Hong Kong, Tat Chee Avenue, Kowloon, Hong Kong*
[c] *Department of Physics, City University of Hong Kong, Tat Chee Avenue, Kowloon, Hong Kong*
[d] *Department of Mechanical and Aerospace Engineering, The Hong Kong University of Science and Technology, Clear Water Bay, Kowloon, Hong Kong*

ARTICLE INFO

Article history:
Received 12 January 2021
Received in revised form
23 July 2021
Accepted 25 August 2021
Available online 31 August 2021

Keywords:
Energy simulation
Green building
Thermochromic smart window
Passive radiative cooler
Passive cooling

ABSTRACT

Thermochromic smart windows and radiative coolers are two passive cooling technologies, whose adoption as windows and roofs, respectively, is feasible for building energy-saving. However, to the authors' knowledge, the investigation of annual energy performance incorporating both techniques is scarce at the time of writing. Therefore, a passive hybrid system involving both technologies is proposed in this study. A perovskite thermochromic smart window and three different radiative coolers were chosen based on their superior performance. The energy performance of the passive hybrid system in a prototypical medium-sized office building was simulated using EnergyPlus and the results were rigorously analyzed. Both thermochromic smart window and radiative cooler could reduce total energy consumptions by up to 10.6% and 23.0%, respectively, regardless of building's year of completion, while the synergic system saved up to 32.0%. Among the chosen cities of various climates, thermochromic smart windows and radiative coolers perform better in cities where cooling demand dominates. The west- and east-facing thermochromic smart windows could mitigate more energy usage in contrast to the other orientations. If this passive hybrid system can be offered at a reasonable cost, the technology is likely to be a viable energy-efficient option for buildings.

1. Introduction

A building envelope consists of windows, roof, and walls. The windows give access to vision and natural ventilation, and provide thermal and visual comfort for the indoor environment [1], while the roof and the walls play an important role in its thermal performance by providing insulation from a harsh outdoor environment. However, these building façades also act as solar collectors or absorbers, causing an increase in the indoor temperature [2]. The heat gained from the external environment and transferred to the inside of the buildings increases air conditioning demand, resulting in substantial energy consumption, particularly in populated hot cities. Air conditioning accounted for 18%, the largest percentage of total energy consumption, in Hong Kong in 2018 [3]. In the same year, space cooling in the US's residential and commercial sectors consumed 380 billion kilowatt-hours (kWh) of electricity, i.e., 10% of the total US electricity consumption [4]. The peak electricity demand will soon be driven by space conditioning, putting a strain on existing electrical power infrastructure, increasing carbon emissions and aggravating global warming and its associated impact on the environment. Therefore, implementing novel technologies requiring zero-energy input to curb this rising cooling energy demand is crucial.

Recently, research on passive cooling technologies which achieve indoor thermal comfort with little to no power consumption, has gained momentum. The two most promising technologies are thermochromic smart windows (TCWs) [2,5] and passive radiative coolers (PRCs) [6]. Li et al. [7] concluded that TCWs, PRCs and personal heat management are three major design guidelines towards a net-zero energy building. TCWs are designed to modulate

* Corresponding author. Department of Mechanical Engineering, The University of Hong Kong, Pokfulam Road, Hong Kong.
E-mail address: cyhchao@hku.hk (C.Y.H. Chao).

https://doi.org/10.1016/j.energy.2021.121914
0360-5442/

Nomenclature

SW	Smart window(s)
DGU	Double glazing unit
TCW	Thermochromic smart window
PRC	Passive radiative cooler
HVAC	Heating, ventilation, air conditioning
VAV	Variable air volume
COP	Coefficient of performance
Pre-1980	Pre-1980 DOE medium-sized office reference building
Post-2010	ASHRAE 90.1−2010 medium-sized office reference building
T_{vis}	Visible transmittance
T_{sol}	Solar transmittance
ΔT_{sol}	Solar modulation ability
R_{vis}	Visible reflectance
R_{sol}	Solar reflectance
T_c	Transition temperature
low-E	Low emissivity
U-value	Thermal conductivity
Ref	Reference
Clear_DGU	Double glazing unit with clear glass only
Low-E_DGU	Double glazing unit with low-E coating
P_25_DGU	Double glazing unit with low-E and thermochromic coatings (T_c at 25 °C)
PRC_Stack	Multilayer TiO_2−SiO_2 passive radiative cooler
PRC_Bio	Bio-inspired PDMS-prism-array-SiO_2-Ag passive radiative cooler
PRC_PDMS	PDMS-SiO_2-Ag passive radiative cooler
P_25_DGU + PRC_Stack	Double glazing unit with low-E and thermochromic coatings (T_c at 25 °C) incorporating multilayer TiO_2−SiO_2 passive radiative cooler

incident solar radiation to reduce heat gain by switching between transmissive and tinted states in response to the ambient temperature. Vanadium dioxide (VO_2) is the most studied material for TCWs because of its fully reversible semiconductor-to-metallic phase transition at the critical temperature, ~68 °C [8]. However, its high phase transition temperature (T_c), low luminous transmittance (T_{vis}), low solar modulation ability (ΔT_{sol}) and intrinsic yellow-brown color are obstacles to practical application. Usage of perovskite for TCWs is an emerging field of study [9−15]. Halder et al. [12] attributed the thermochromism of a kind of perovskite to the reversible hydration/dehydration process of $CH_3NH_3PbI_3$ when it encounters moisture. Therefore, a TCW with lead halide perovskite thin film was proposed [13]. The lead halide perovskite $CH_3NH_3PbI_3$ smart coating switches from clear to tinted state as it loses water molecules through dehydration (heating) and returns to clear state by hydration (cooling). The results show better performance over traditional VO_2 TCWs in terms of a higher ΔT_{sol}, a higher T_{vis} and a lower T_c.

PRCs provide cooling by simultaneously reflecting the solar radiation to reduce heat gain and emitting infrared radiation within the earth's atmosphere transparent window (in the region of wavelength from 8 to 13 μm) to the outer space to promote heat dissipation. In practice, water vapor and other gases like CO_2 in the atmosphere which emit long wave radiation; and cloud cover which blocks outgoing radiation are detrimental to the PRCs' cooling performance. Recent PRC technologies that have been investigated include multilayer stacks [16−18], and nanophotonic structures/metamaterials [19−26]. The multilayer structures as well as nanophotonic structures require a high degree of precision and are expensive and complex to fabricate, thereby limiting scalability. Therefore, some simple materials which have high emissivity in wavelengths from 8 to 13 μm have also been selected to construct radiative coolers [27].

The benefits of implementing passive cooling technologies can be quantified by building an energy model using simulation tools [28,29]. Saeli et al. [30] conducted the first such study of TCWs using EnergyPlus to evaluate the energy consumption of four TCWs in different cities and discovered that the TCWs performed best in warm climates. A similar study by Hoffman et al. [31] found 3.1−12.5% less annual energy use with TCW compared to commercial low-emissivity (low-E) windows. However, some research [32] stated that the emissivity of a window plays a bigger role in energy saving compared to ΔT_{sol}. Therefore, these contradictory findings necessitate further research. The PRC technologies reported in literature perform remarkably well under controlled laboratory conditions and field tests. However, there is limited data available on the energy-saving potential of available daytime radiative cooling technologies in buildings in year-round applications, under different climatic conditions. Using EnergyPlus, Li et al. [33] found that delignified wood, a passive radiative cooling wood, achieves an average cooling energy saving of ~20% for new midrise apartment buildings in the United States. The photonic radiative cooler developed by Raman et al. [17] showed a 1.185 × 10^5 kWh electricity annual saving for a medium sized commercial building in Phoenix, Arizona. The scarcity of performance data of available cooling technologies in different climates (especially outside the United States) is a hurdle before practical application especially since PRCs are known to be adversely affected by weather conditions.

The studies mentioned above demonstrated that TCWs and PRCs individually can achieve promising performance in some cases. However, there is a lack of studies on an integrated hybrid system with both TCWs and PRCs installed in a building. Therefore, this study aims to investigate the estimated energy saving with the application of such a passive hybrid cooling system. First, the energy-saving performance for perovskite TCW [13] and three PRCs [18,26,27] reported in literature was investigated under various climates using EnergyPlus. The first PRC is a multilayered cooler (PRC_Stack), the second PRC is a bioinspired-nanophotonic cooler (PRC_Bio), and the last PRC is a cooler based on a cheap material and an easy fabrication method (PRC_PDMS). The materials that were selected for the simulation are summarized in Table 1. This paper aims to address: 1. The energy-saving potential of a hybrid passive system with respect to different climates and end-use categories (heating, cooling, lighting and fan); 2. The feasibility of hybrid passive systems in both older buildings (pre-1980) as well as new buildings (post-2010); 3. Which orientations are better for installing the perovskite TCWs; 4. The relative energy savings contribution of TCWs versus conventional technologies (i.e., low-E); 5. Any secondary effects of PRC roof integration (heating/ventilation energy consumption).

2. Methodology

2.1. Climates of chosen cities

The cities for energy simulations (Hong Kong, New York, Singapore, Cairo, and Rome) were selected to represent four main

Table 1
Thermochromic smart windows and passive radiative coolers chosen for EnergyPlus simulation.

Type of Technology	Comments	Abbreviation	Ref.
Thermochromic Smart Window	Perovskite Smart Window, $CH_3NH_3PbI_3$	P_25	[13]
Passive Radiative Cooler	Multilayered TiO_2–SiO_2 cooler, 4 alternating layers of TiO_2–SiO_2	PRC_Stack	[18]
Passive Radiative Cooler	Bio-inspired cooler, PDMS Triangular Prism Array on silica mirror	PRC_Bio	[26]
Passive Radiative Cooler	PDMS cooler, PDMS – SiO_2–Ag	PRC_PDMS	[27]

climate groups of the Köppen climate classification: tropical (A), dry (B), temperate (C), and continental (D) [34]. Table S1 in the Supplementary Materials shows the climate types of the cities chosen for this study. The performance of perovskite TCWs and PRCs evaluated for the different climate zones can be extended to similar conditions in other geographical locations. The polar climate type, with average annual temperatures less than 10 °C, was disregarded as it would not benefit from passive cooling technologies.

2.2. Simulation model

The energy-saving potential of the passive cooling technologies is estimated in reference to a medium-sized office building [35]. The detailed medium-size office building model is described in Note S1 in Supplementary Materials.

A perovskite thermochromic window proposed by Zhang et al. [13] was investigated in the simulation study. The thermochromism of the perovskite glazing is attributed to a hydration/dehydration process and therefore the T_c can be tuned by controlling the relative humidity. For the purpose of this paper, thermochromic glazing with a T_c of 25 °C was considered: when the temperature of the glazing material exceeds 25 °C, it switches from a clear to tinted state reversibly. This glazing material will hereinafter be referred as P_25.

Traditional clear glass panels have been widely replaced by double-glazed units (DGUs) with low-E coating on one of the panels (low-E_DGU) in many architectures, especially commercial high-rise buildings. low-E glass has low emissivity compared to conventional clear glass and selectively reflects part or all types of infrared radiation, minimizing the heat dissipation in winter and minimizing the solar heat buildup in buildings in summer while providing high T_{vis} [36]. To maximize the thermal efficiency of the modeled building, the TCW was modeled as a DGU incorporating both P_25 and low-E layers (see Fig. S3 in Supplementary Materials). These perovskite DGUs (P_25_DGU) were modeled with the thermochromic layer facing outside (outboard layer) in order to minimize the transmission of absorbed radiation indoors. A commercially available low-E coating with 0.068 emittance was selected for the inboard glazing layer. A traditional clear glass DGU (Clear_DGU) was defined as the baseline model which serves as the reference to assess the energy savings using TCWs. Additionally, a building outfitted with simple low-E_DGUs was modeled to evaluate the relative energy savings contribution of low-E_DGUs and TCWs. The configurations of the P_25_DGU and reference glazing units are displayed in Table 2. The transmittance and reflectance spectra reported in publications were used to derive the optical properties of the P_25 in its clear and tinted state. The glazing units were then modeled with thermally broken aluminum frames using WINDOW 7.7 [37]. The thermal and optical performance indices of these units are reported in Table S2 in the Supplementary Materials.

The dynamic window properties were modeled using the dedicated module from EnergyPlus 9.2 for thermochromic glazing [38]. This module allows user to define the thermochromic glazing properties at different temperatures; when the simulation is run, the glazing layer switches between the hot (tinted) and cold (clear) states depending on its surface temperature. The model considers heat transfer across the building envelope and internal loads due to occupants, interior lighting and equipment, to solve the glazing layer heat balance equation and determine its temperature at a given instance. Optical properties corresponding to the closest temperature in the user-defined input are then assigned to the window. These calculations are performed iteratively with a timestep of 1 min.

The implementation of TCWs is expected to have a negative effect on the lighting load, as the decreased T_{vis} of the tinted state of the window gives rise to the need for compensatory lighting indoors. Therefore, changes to the lighting energy were analyzed in addition to cooling and heating energy. The energy savings reported for the four perimeter zones were used to study the effect of orientation on TCW performance. Since the post-2010 building model utilizes a centralized space conditioning system, the energy consumption for cooling and heating for the individual zones were calculated as a ratio of the airflow rate at the duct air terminal of the respective zones. The cooling and heating energy consumption reported by EnergyPlus is the electricity used to power the heating and cooling coils of the HVAC system. The energy used for the ventilation system, which moves the cold/hot air to the vents through the duct system, is reported under the end-use category “Fan”.

The ideal daytime PRC material has unity emissivity in the atmospheric window (8–13 μm) and unity reflectance of all other wavelengths in order to harness outer space's potential as a heat sink. The PRCs used in the simulation include a multilayer structure, a polymer-based cooler and a biomimetic structure. The reasons for choosing these three PRCs are explained in Note S2 in Supplementary Materials.

The proposed radiative cooling system works independently of the building's existing cooling infrastructure. A rooftop heat exchanger hydronic loop is used to harness and deliver the cooling energy provided by the radiative cooling roof panels to supplement the existing Variable Air Volume (VAV) system. This element is modeled as an additional cooling coil which is integrated with the HVAC system with minimal interference to the operation of the

Table 2
Configuration of Reference and Thermochromic Glazing Systems used in the Simulation.

Glazing System	Layer 1 (Inboard)	Gap	Layer 2 (Outboard)
Reference (Clear_DGU)	Clear Glass	90% Argon, 10% Air	Clear Glass
low-E Glazing Unit (Low-E_DGU)	low-E Glass	90% Argon, 10% Air	Clear Glass
TC Glazing Unit (P_25_DGU)	low-E Glass	90% Argon, 10% Air	Thermochromic film (Perovskite)

existing cooling apparatus. The energy simulation model modifies the building's existing construction by adding the radiative cooler on the roof membrane. To do so, the PRC was modeled as a building material. The optical properties were calculated by the equations in Note S3 and Table S3 in Supplementary Materials.

EnergyPlus does not support a dedicated module for radiative coolers. Therefore, EnergyPlus's energy management system (EMS) framework was used to create a custom model to calculate the cooling energy available from the PRC and the consequent cooling electricity savings at each timestep of the simulation. The simplified model is explained in Note S4 in Supplementary Materials. For each timestep of the simulation, the equivalent electric power of the useful cooling energy generated by the radiative cooling panels is derived by dividing this value by the COP (coefficient of performance) of the refrigeration system. The cumulative savings make up the annual cooling energy consumption improvement. The assumptions and the limitations are clarified in Note S4 in Supplementary Materials.

3. Results and discussion

3.1. Effect of model construction on energy savings

The energy consumption with P_25_DGU and PRCs employed individually will be discussed in this section, followed by the energy consumption of the hybrid passive cooling system. As expected, pre-1980 constructions consume significantly more energy annually than the newer constructions (Fig. 1) as a result of the more stringent requirements that newer models (Post-2010) must comply to. For instance, the insulated steel frame walls of the pre-1980 and post-2010 models have thermal resistance of 1.56 and 3.47 m^2 K/W respectively. This results in better thermal insulation in the newer buildings, and consequently less heating/cooling energy wastage. Additionally, the pre-1980 model is outfitted with lights that consume 16.9 W/m^2, against the much more energy-efficient (9.70 W/m^2) lights in the post-2010 model. Also contributing to the higher energy use in the pre-1980 model, are the individual HVAC loops that serve each zone instead of floor specific HVAC systems characteristic of the post-2010 building model. The detailed definitions of pre-1980 model and post-2010 model are described in Note S1 in Supplementary Materials.

Despite this difference in the absolute values for energy use between the two models, the overall energy savings of the different window technologies, and the trends in energy saving potential are comparable. For all cities and both pre-1980 and post-2010 models, the energy saving values using P_25_DGU are larger than low-E_DGU. The focus hereinafter (in the section dedicated to the TCW) will be the energy savings calculated for the post-2010 model, as the conclusions drawn for one construction type are pertinent to the other.

Fig. 2 summarizes the percentage energy improvement by three different PRCs in each of the five cities for pre-1980 and post-2010 models. The effect of implementing PRC is more evident in the newer buildings. PRC_Stack consistently outperformed other PRCs, with the energy-saving potential sequentially decreasing for PRC_Bio and PRC_PDMS in all cities. The implementation of a PRC system influences the energy consumption of multiple HVAC components, namely the chiller, and secondarily the fan, which circulates hot/cold air to achieve the thermostat set point temperature; and heating unit. The three end-use categories will be reviewed in the following section.

The installation of radiative cooling material on the exterior surface of the building roof is expected to save energy by (1) reflecting incident solar radiation and radiating mid-infrared radiation, thereby cooling the roof and (2) generating cooling power to supplement the existing HVAC system. The cooling savings depicted in Fig. 2 is a sum of the passive cooling effect achieved by simply applying the radiative cooling material (referred to the (1) mechanism above, and captioned as "cooling roof"), and the cooling using the chilled water loop (referred to the (2) mechanism above, and captioned as "circulated loop"). It is evident that the contribution of "cooling roof" is more significant in older buildings (illustrated in Fig. 3). This trend could be attributed to the low solar absorptance (A_{solar}) value of the radiative cooling material compared with the existing pre-1980 roof membrane. The pre-1980 office building has a conventional dark roof, with A_{solar} of 0.7. When the PRC is applied, the roof's solar absorption property is compromised, and the passive cooling effect is magnified. The more recent ASHRAE 90.1–2010 standards, however, dictate the roof to be made of a highly reflective (A_{solar} of 0.45) material, therefore the passive cooling savings are more muted as the PRC material offers less improvement in terms of cool roof behavior. Moreover, upgraded roof insulation in newer buildings (IEAD-insulation entirely above deck-R-20.83 versus IEAD R-10.0 in pre 1980

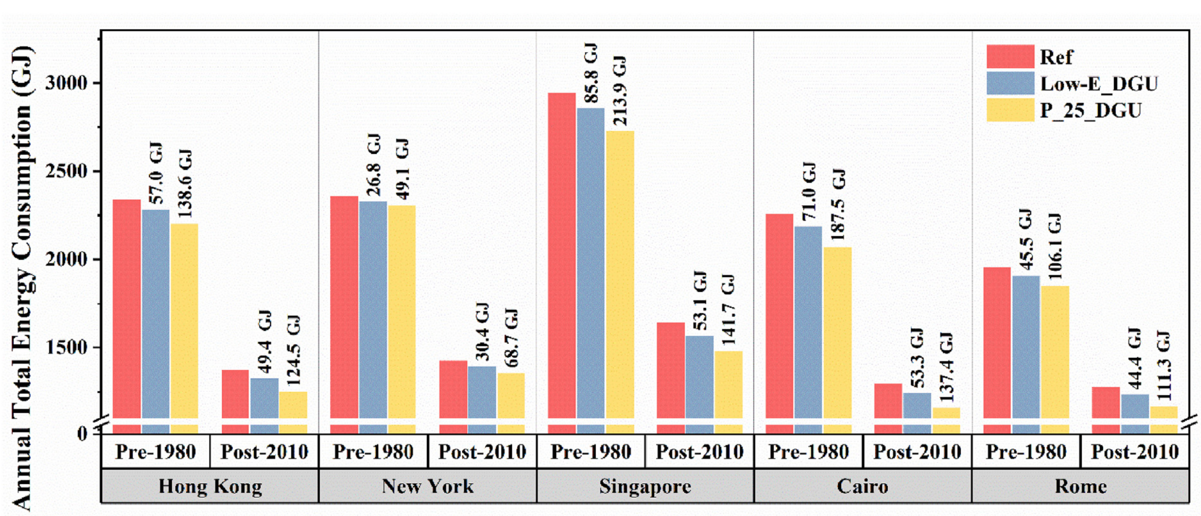

Fig. 1. Annual total energy consumption and annual total energy savings for pre-1980 and post-2010 buildings using low-E_DGU and P_25_DGU with respect to Clear_DGU. Labels above columns represent absolute energy reduction with the respective glazing units.

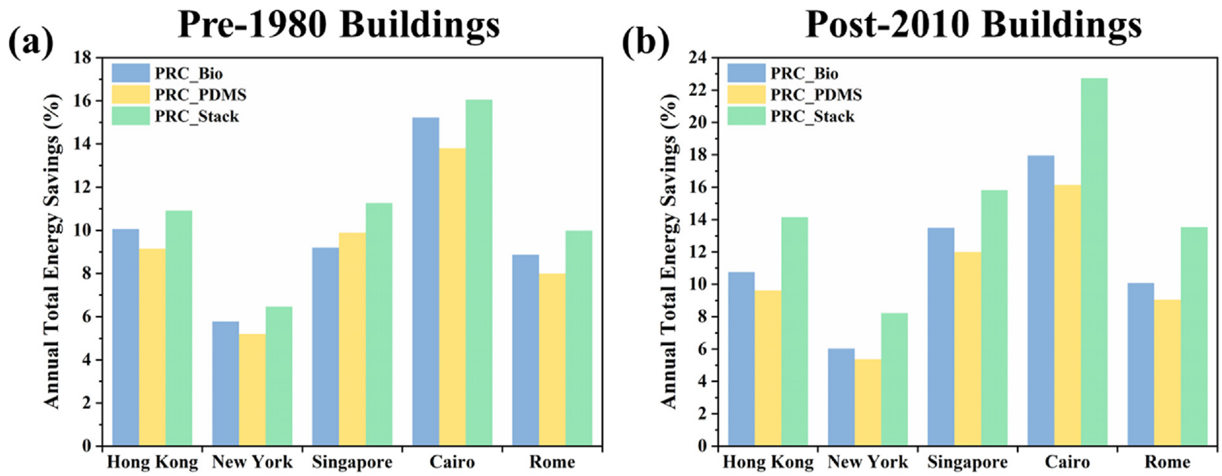

Fig. 2. Total energy savings in (a) Pre-1980 and (b) Post-2010 buildings with different PRC.

constructions) inhibits the transfer of this passive cooling effect to the cooled space indoors.

3.2. Effect of climate on energy savings

The low-E_DGUs save energy by thermally insulating the windows, minimizing the radiant heat gain and heat loss during the cooling and heating period, respectively. It is evident from Fig. 1 that P_25_DGUs were more energy-efficient than static low-E_DGU. The combination of the low-E inboard layer and the thermochromic glazing offer improved energy savings than when the low-E layer was used by itself. This even holds true in cold climates. In New York, where energy-saving potential is limited due to the colder weather, the buildings saved 68.7 GJ energy. The effect of P_25_DGUs was more apparent in cities that have warmer climates with the greatest energy saving of 137.4 GJ in Cairo. The positive correlation between the climatic temperature and the absolute cooling savings could be attributed to the increased instances of glazing switching in warmer conditions. It is more likely that the ambient temperature exceeds the thermochromic material's T_c in hotter climates, prompting the glazing to switch more frequently. As a result of increased tinted hours, the reduction in heat gain through the windows, ergo cooling load, is more significant. The effect of TCWs on the glazing's energy performance by energy end-use category is summarized in Fig. 4.

TCWs save energy during the cooling period (in summer) by regulating the heat gain through the building envelope. In its tinted state, the TCWs have low solar transmittance (T_{sol}) which impedes the passage of incident radiant flux through the window (direct heat gain). Ideally, this short-wave radiation is totally reflected instead. In practice, however, non-zero absorptance of the window is impossible to achieve. This is detrimental to the smart window's cooling energy savings because it facilitates passive heating of the interior (indirect heat gain) when the absorbed solar radiation is transferred to the building space via conduction, convection and radiation. The P_25_DGU has lower T_{sol} in both its clear and tinted states (0.5406/0.3328) compared to the low-E_DGUs (0.5965), i.e., the P_25_DGU has lower direct heat gain which is desirable for cooling savings. However, the solar absorptance (A_{solar}) of P_25_DGUs (0.3040 for hot state) is higher than that of low-E_DGU (0.1054). Despite this, the switchable TCWs offered more savings in cooling.

In many of the cities studied, the P_25_DGUs saved heating energy. For instance, P_25_DGUs saved heating energy by 22.38% (24.23 GJ) in Hong Kong. This may be attributed to the low-E layer in P_25_DGUs. The low-E coatings minimized the radiant heat lost to the surroundings: long wave heat radiation from the heated space is reflected back inside by the low-E layer. This reduces the strain on the HVAC system which does not have to work as hard to maintain the heating set point temperature of 21 °C. Therefore, it is

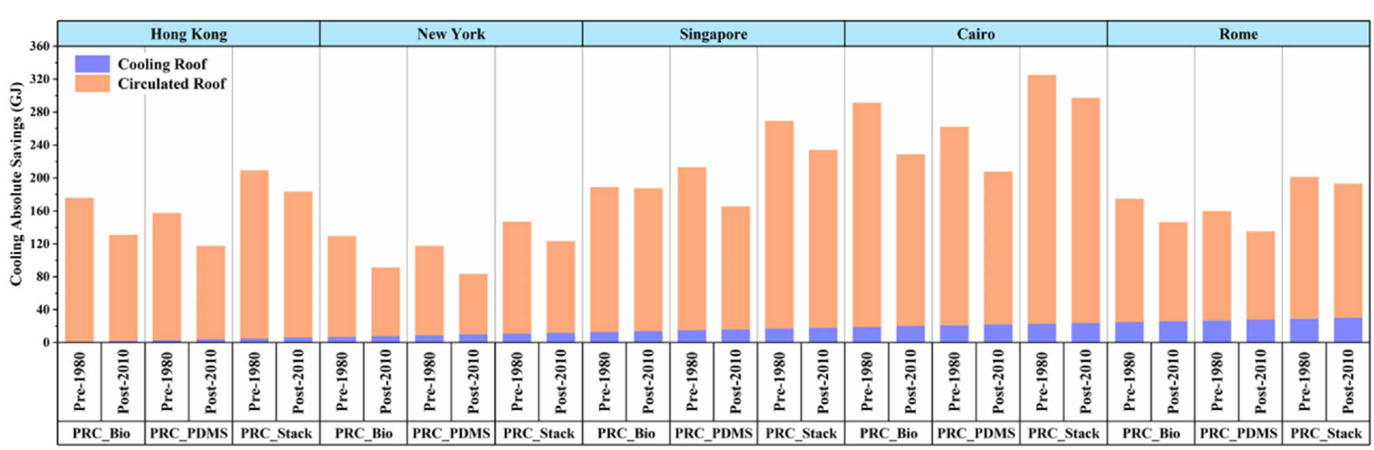

Fig. 3. Useful cooling energy generated by PRC in (a) Pre-1980 ad (b) Post-2010 buildings.

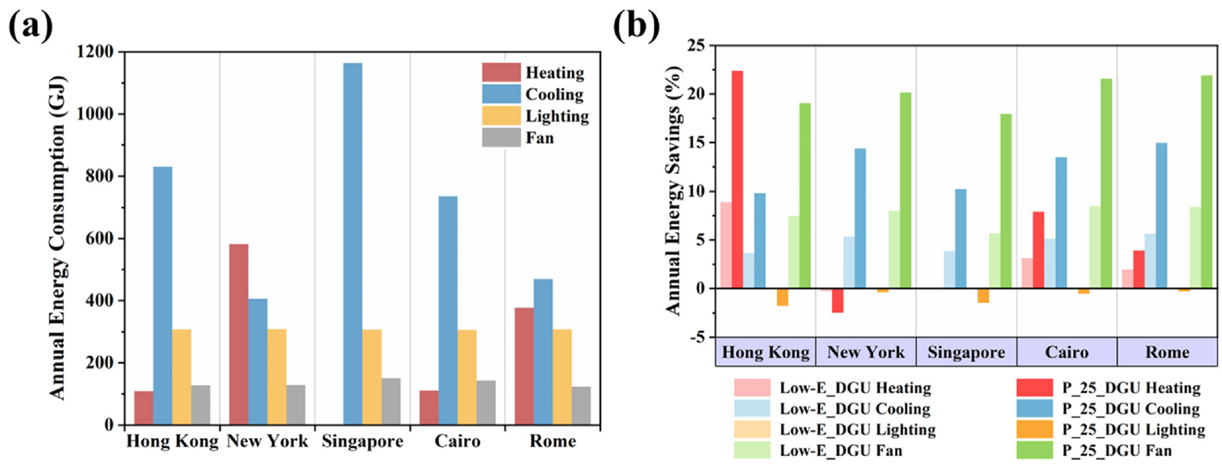

Fig. 4. Annual energy consumption for (a) reference model (Clear_DGU) by usage and (b) Annual energy savings in each usage with Low_E_DGU and P_25_DGU in post-2010 buildings.

reasonable that the P_25_DGU which has a low-E layer on the inner panel can save heating energy. However, P_25_DGU saves more heating energy than low-E_DGU due to higher indirect heat gain by higher A_{solar} of the P_25_DGU. This interesting phenomenon is under a detailed analysis and will be presented in our future work.

The drawback of implementing TCWs is the increased opacity of the glass compared to the base model (Clear_DGUs). The T_{vis} of the P_25_DGUs in the clear and tinted state is 0.7212 and 0.2404, respectively, against 0.8143 for the Clear_DGUs and 0.7936 for the low-E_DGUs. In buildings where the lighting is automated to follow a pre-set luminaire schedule by continuous light dimming/brightening, lighting energy use increases when TCWs are tinted. Between ~0.5 and ~2% increase in the lighting was observed with P_25_DGUs. The low-E_DGUs also showed a consistent increase in the lighting demand (approximately 0.05% in all cities) because the commercially available low-E glazing chosen for the study has a slightly tinted hue (T_{vis} of 0.7936) which impedes the transmission of incident visible light. As expected, the increase in lighting energy use is inversely proportional to the transmittance, i.e., the lower the T_{vis}, the higher the lighting demand increase. For the medium-sized office building that is the subject of this study, the lighting demand in the perimeter zone, which skirts a windowless core zone, only accounts for ~10% of the total lighting energy. Since the switching behavior of the dynamic window units affects the lighting in this region exclusively, the negative effect on the energy consumption is not very significant. The usage increase for thermochromic windows varied by region. The increase is comparatively higher in cities with hotter temperatures (still, the increment is lower than 1.8%). This is rationalized by the higher tinted hours in these climates because the glazing temperatures exceed its T_c more often.

By reducing the cooling/heating load on the space conditioning system, the strain on ventilating components of the HVAC loop is alleviated, in addition to the heating/cooling elements. Similarly, when the cooling/heating load increases, these components' energy use is negatively affected. Therefore, the ventilation savings is reflective of both the savings and negative effects of the smart windows. The consumption improvement indicates net positive results, with comparable savings calculated for different cities (~20% using dynamic P_25_DGUs, ~7.5% using low-E_DGUs).

There is no on/off control for the "cooling roof effect" of PRCs; i.e., it is available all year round. Although this is beneficial during the cooling period (summer), it can result in an energy usage penalty during the heating period (winter). Conversely, the "circulated" cooling energy can be regulated as required to prevent unwanted cooling during the winter. The "circulated" cooling capacity of PRCs is more substantial in hotter and drier climates. For instance, maximum cooling energies of 273.44 GJ (post-2010), were generated by PRC_Stack in Cairo against more modest 111.27 GJ (post-2010) in New York (shown in Fig. 5). This is consistent with expectations since Cairo has the lowest average humidity of the cities in the simulation study. To maximize the cooling potential of the PRC, low atmospheric humidity (i.e. low sky emissivity), is key. Water molecules absorb specific wavelengths of outgoing long wave radiation, therefore excess humidity makes the atmospheric window less transparent. Moreover, outgoing radiation is backscattered to earth by atmospheric constituents like water vapor. The device's net emissive power is limited as a result of the elevated atmospheric thermal radiation, i.e., there is a negative effect on the cooling power generated by the PRC. The long winters and the relatively lower temperatures limit the PRC's performance in cold climates comparable to New York and Rome.

The energy-saving capability of the proposed system is limited as it is designed to provide *in situ* cooling using the radiative panels installed on the roof. By introducing cold storage infrastructure, the unused nocturnal cooling flux can be stored in chilled water tanks and used when the instantaneous cooling power of the PRC system is unable to meet the cooling demand by itself during the day, further reducing reliance on the mechanical chiller unit. Realistically, coverage of the entire roof with the radiative panels is not possible, as it usually houses HVAC equipment, skylights and other machinery in addition to walkways and screens to allow for their servicing, maintenance and protection. Simulations of cases with half of the roof area utilized for radiative cooling showed ~50% fewer cooling savings, i.e., an approximate direct linear proportionality exists between the radiative area and the energy savings. For example, doubling the PRC coverage area increases the active cooling energy savings from 151.76 GJ to 273.4 GJ in Cairo using PRC_Stack. Similar to cooling, the fan end-use showed energy savings, albeit much smaller percentage changes averaging 1.68% (post-2010) for 100% roof coverage.

Despite energy saving when cooling is required, the reduced solar heat gain is detrimental during the winter, as evidenced by the increase in heating energy consumption for all cities (smaller than 4% in all cities for all coolers in a post-2010 buildings model). In addition to the muted absorptance of PRCs relative to the roof material, their thermal conductivities are higher. The lower absorptance decreases the passive indoor heat gain through the roof; the high thermal conductivity promotes heat dissipation

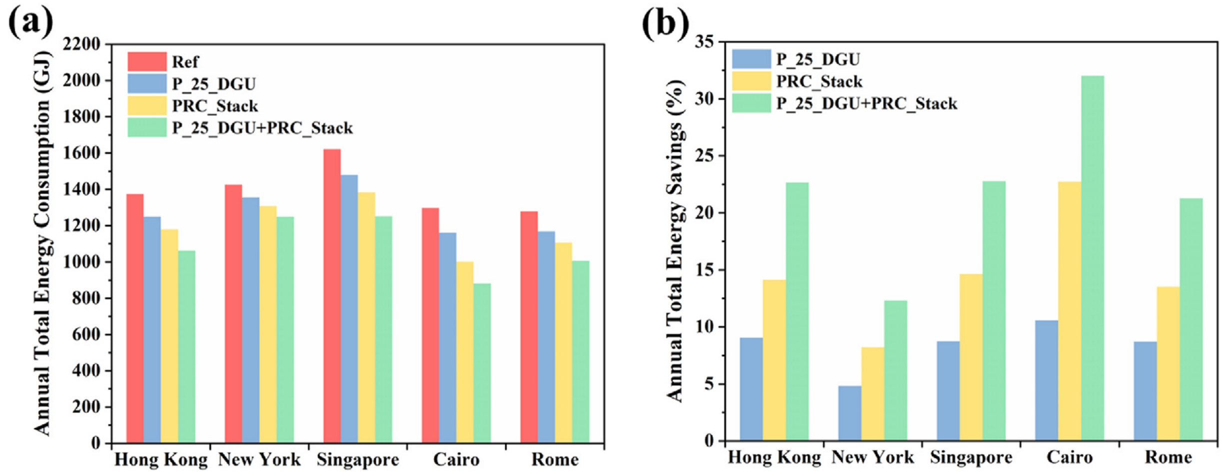

Fig. 5. a) Annual energy consumption and b) Annual total energy savings with different technologies in post-2010 buildings.

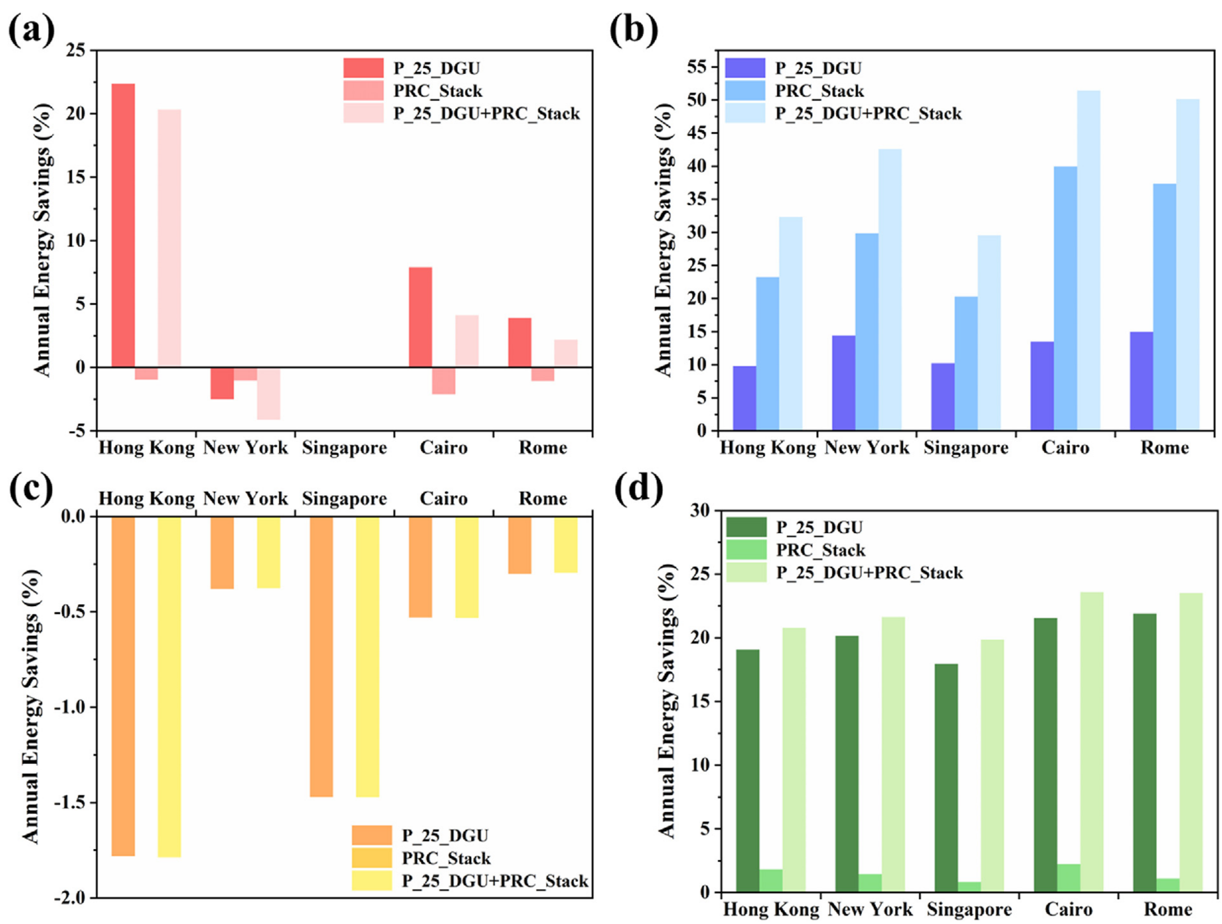

Fig. 6. Annual energy savings of (a) Heating, (b) Cooling, (c) Lighting and (d) Fan in each city using P_25_DGUs, PRC_Stack, and P_25_DGUs + PRC_Stack in post-2010 buildings.

across the building envelope increasing heating wastage.

It must be taken into account that the model assumes unidirectional emission of the planar roof radiators. In practice, however, the radiation from the device is omnidirectional, which means that its cooling performance is heavily influenced by surrounding architecture and unhindered access to the sky. For very tall buildings, clear skies are more accessible. For medium-sized buildings in urban canyons, such as the one considered in the study, this is more of a challenge as radiative emissions are blocked by neighboring buildings that are taller. Therefore, the effect of the building's surroundings must be factored in for a more realistic result.

To further minimize the solar heat gain through building facades, a passive hybrid system containing both P_25_DGU and PRC_Stack (PRC_Stack was chosen for its optimal energy saving capacity among three PRCs) was implemented in post-2010 buildings to investigate the effectiveness in energy saving. The energy saving increases in the order of P_25_DGU, PRC_Stack and P_25_DGU + PRC_Stack with respect to Clear_DGU, as depicted in Fig. 5. The total energy consumption ranges from 882 GJ to 1255 GJ, with Cairo consuming the least energy and New York the most. P_25_DGU + PRC_Stack exhibited the greatest saving of 32.0% (415 GJ) in Cairo and lowest of 12.4% (177 GJ) in New York. The total energy usage in Hong Kong and Singapore with hot and humid weather improves by about a quarter. As the gross surface area of roof of the medium-sized office building for this study is approximately 1661 m^2, which is about 2.5 times the total gross area of window, P_25_DGU + PRC_Stack pronouncedly tripled energy savings compared to applying P_25_DGU alone in each city.

The application of P_25_DGU + PRC_Stack discouraged energy savings in heating in New York (as shown in Fig. 6(a)), which could be the result of utilizing materials that reflect solar radiation. The savings in cooling energy were boosted to 51% from 13% (with P_25_DGU only) in Cairo, followed by 50% in Rome and lowest savings of 30% in Singapore. Lower percentage improvement could be attributed to larger base values of cooling energy use in Singapore and Hong Kong than in other cities. The addition of

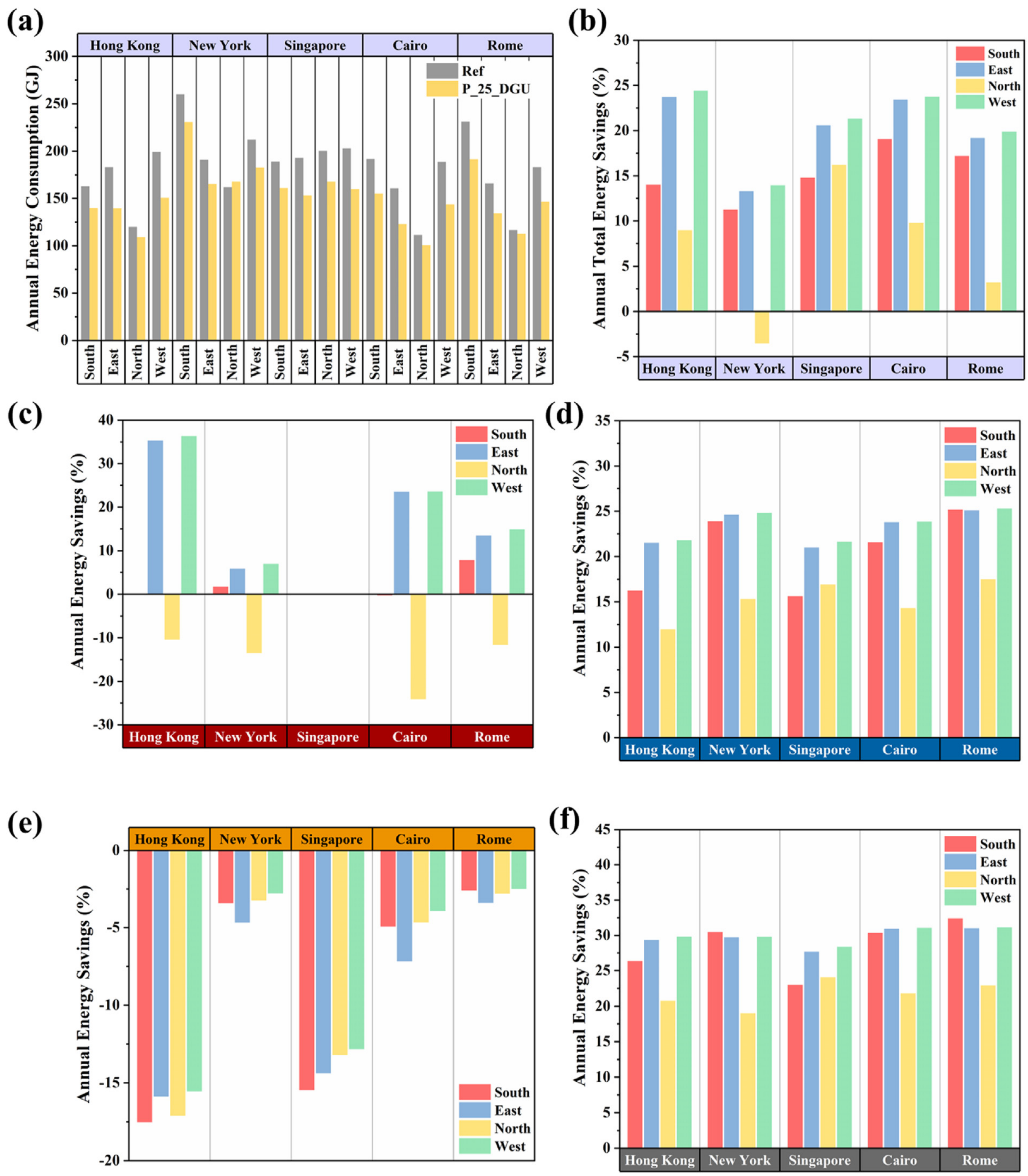

Fig. 7. (a) Annual energy consumptions, (b) Annual total energy savings and in (c) Heating, (d) Cooling, (e) Lighting and (f) Fan, for each city at each perimeter zone (south, east, north and west) using P_25_DGUs in post-2010 buildings.

PRC_Stack does not impact lighting energy in buildings with P_25_DGU (as shown in Fig. 6(c)). Energy consumption for ventilation reduced in all cities, with the greatest improvement of 24% in Cairo and lowest of 20% in Singapore by P_25_DGU + PRC_Stack.

3.3. Effect of orientation on energy savings

Thermal comfort and air ventilation of a building, which is driven by natural elements such as the intensity of solar radiation, wind patterns, seasons and temperature variations are highly associated with orientation [39]. Architectures built at suitable orientations can exploit these conditions for passive heating and cooling, improving energy efficiency and thermal comfort, and reducing energy cost. Orientation has no effect on the performance of PRCs. Therefore, in this section, only TCWs are discussed. The switching behavior of the TCWs is affected by its daylight accessibility. Hence, in order to rationalize the energy savings trends, it is important to consider the daily and seasonal sun trajectory. The cities considered in the study are in the northern hemisphere where the sun culminates in the south (Fig. S4 in the Supplementary Materials).

The annual energy consumptions (in GJ) and the overall energy consumption savings (%) for four orientations in different climates are illustrated in Fig. 7(a) and (b), respectively. In New York, the total energy use in the north-facing zone increased with TCWs: the heating energy penalty outweighs all other savings. This emphasizes the importance of forfeiting TCWs in north-facing zones for cities in the northern hemisphere with long and harsh winters. It is noteworthy however that the perimeter zones of the medium-sized office are non-identical. The northern and southern zones, which form the building's length-wise border, are much larger, with a total window area of 19.58 m^2 against 13.06 m^2 of the east and west zones. Moreover, the solar altitude increases with decreasing latitude of the cities: this affects solar access. The authors caution that these variables may introduce slight discrepancies in the observed trends.

Due to the sun path in the northern hemisphere (described in Note S4 in Supplementary Materials), the east- and west-facing windows receive the most solar heat gain and glare, and thus increased tinted hours. This manifests higher cooling savings, which is supported by the percentage savings by end use data in Fig. 7(d). Objects (streets, pavements, buildings etc.) collect heat throughout the day resulting in higher temperatures in the afternoon when the sun is in the west. They radiate heat leading to higher window temperatures. Therefore, the west-facing windows report marginally longer tinted hours, and better cooling energy savings than the east. The cooling energy improved by 21.86% in the western zone (the largest improvement spanning all zones) in Singapore, against 21.27% in the eastern zone. This trend is mirrored in the fan end use improvement data (Fig. 7(f)).

All perimeter zones except for the north-facing zone recorded heating energy savings with the implementation of P_25_DGUs (Fig. 7(a)). This may be due to the higher indirect absorptive heat gain by P_25_DGU (higher A_{solar}). During the heating period (winter) the south-facing windows received most of the winter sun, with the windows of the northern zones getting the least solar heat gain of all orientations, as a result of the day-arc discussed above. Limited solar radiation produces insufficient indirect heat gain by P_25_DGUs. Therefore, it is not advisable to implement north-facing TCWs in cities in the northern hemisphere.

The luminaire schedule for the daylighting controls must be factored in when analyzing the effect of orientation on the lighting energy use. Despite the increased tinted hours of the west-facing space as a result of the intense solar radiation and high mid-afternoon temperatures, the western zone shows the smallest lighting use increase of all orientations (Fig. 7(e)). When the western zone is exposed to the sun (mid-afternoon), the lighting demand is very small since the operational hours of the building are from 0800 to 1600. Sunlight through the window fulfills this demand without significant help from artificial lighting. Therefore, whether the windows exist in the clear or tinted state makes little difference to the lighting energy consumption (even in tinted state, the natural illuminance is enough).

For practical application, it is important to offer the techniques at a reasonable price compared to the energy they can save. The cost of the techniques mainly comes from the raw materials and fabrication process. All radiative coolers use a noble metal, silver, to reflect solar radiation. However, silver can be replaced by a cheaper metal like aluminum by further structure optimizations. Perovskite smart windows do not require expensive raw materials. The fabrication process for perovskite smart window and PRC_PDMS is simple and cheap, since it only involves the spinning coating process. However, PRC_Stack and PRC_Bio are difficult and expensive to fabricate even in lab environment since they both involve multiple photolithography processes. Further price reductions in the unit cost can be expected in industry-scale mass production.

4. Conclusion

The year-around performance of P_25_DGU, three different PRCs and a passive hybrid system (P_25_DGU + PRC_Stack) in pre-1980 and post-2010 medium-sized office buildings and the energy savings with respect to Clear_DGU were investigated using EnergyPlus. Retrofitting or installing P_25_DGU in the old and newly-constructed buildings can both reduce building energy consumption. The implementation of P_25C_DGU has a more pronounced effect in cities where cooling demand dominates and improved total energy consumption by up to 10.6%. The perovskite coating with darker appearance than conventional window influences the T_{vis} of P_25_DGU, leading to a slight increase in lighting energy. P_25_DGU shows greatest energy saving potential in the east- and west-facings, while they are not recommended to be adopted as the north-facing glazing in cold cities. Among the three types of PRCs, PRC_Stack shows outstanding energy savings of 8%–23% with the greatest saving in Cairo. Applying P_25_DGU with PRC_Stack in the building models drastically improves total energy use by 12%–32% in the chosen cities. Future work should explore how building types and window-to-wall ratio influence the performance of passive technologies. Parametric studies of thermochromic smart window properties, in particular, its transition temperature will be conducted to further enhance its applicability. Moreover, the fabrication processes of these technologies should be exhaustively investigated as the cost and scalability should be optimized for mass production and deployment. This study demonstrated that using a hybrid passive system including P_25_DGU and PRC can promisingly save energy usage in office buildings in all climates.

Credit author statement

Yi Zhang: Conceptualization, Methodology, Writing – original draft. **Thilhara Tennakoon**: Methodology, Investigation, Writing – original draft. **Yin Hoi Chan**: Methodology, Validation, Writing – original draft. **Ka Chung Chan**: Resources, Writing – review & editing. **Sau Chung Fu**: Data curation, Writing – review & editing. **Chi Yan Tso**: Project administration, Funding acquisition. **Kin Man Yu**: Project administration, Funding acquisition. **Bao Ling Huang**: Project administration, Funding acquisition. **Shu Huai Yao**: Project administration, Funding acquisition. **Hui He Qiu**: Project administration, Funding acquisition. **Christopher Yu Hang Chao**: Supervision, Project administration, Funding acquisition.

Declaration of competing interest

The authors declare that they have no known competing financial interests or personal relationships that could have appeared to influence the work reported in this paper.

Acknowledgement

The work was supported by the Collaborative Research Fund (CRF) (project no. C6022-16G) from the Research Grants Council of the Hong Kong Special Administrative Region, China.

Appendix A. Supplementary data

Supplementary data to this article can be found online at https://doi.org/10.1016/j.energy.2021.121914.

References

[1] Gopi S. Basic civil engineering. Pearson Education India; 2009.
[2] Rezaei SD, Shannigrahi S, Ramakrishna S. A review of conventional, advanced, and smart glazing technologies and materials for improving indoor environment. Sol Energy Mater Sol Cell 2017;159:26–51.
[3] Electrical and Mechanical Services Department (EMSD) Hong Kong. Hong Kong energy end-use data 2020. Aug. 8, 2020. https://www.emsd.gov.hk/en/energy_efficiency/energy_end_use_data_and_consumption_indicators/hong_kong_energy_end_use_data/data/. [Accessed 3 October 2020].
[4] U.S. energy information administration, U.S.. Energy Facts explained. May 7. 2020. https://www.eia.gov/energyexplained/us-energy-facts/. [Accessed 3 October 2020].
[5] Tällberg R, Jelle BP, Loonen R, Gao T, Hamdy M. Comparison of the energy saving potential of adaptive and controllable smart windows: a state-of-the-art review and simulation studies of thermochromic, photochromic and electrochromic technologies. Sol Energy Mater Sol Cell 2019;200:1–30.
[6] Santamouris M, Feng J. Recent progress in daytime radiative cooling: is it the air conditioner of the future? Buildings 2018;8(12):168.
[7] Li X, Xie W, Sui C, Hsu P-C. Multispectral thermal management designs for net-zero energy buildings. ACS Mater Lett 2020:1624–43.
[8] Morin F. Oxides which show a metal-to-insulator transition at the Neel temperature. Phys Rev Lett 1959;3(1):34.
[9] De Bastiani M, Saidaminov MI, Dursun I, Sinatra L, Peng W, Buttner U, Mohammed OF, Bakr OM. Thermochromic perovskite inks for reversible smart window applications. Chem Mater 2017;29(8):3367–70.
[10] Lin J, Lai M, Dou L, Kley CS, Chen H, Peng F, Sun J, Lu D, Hawks SA, Xie C. Thermochromic halide perovskite solar cells. Nat Mater 2018;17(3):261–7.
[11] Wheeler LM, Moore DT, Ihly R, Stanton NJ, Miller EM, Tenent RC, Blackburn JL, Neale NR. Switchable photovoltaic windows enabled by reversible photothermal complex dissociation from methylammonium lead iodide. Nat Commun 2017;8(1):1–9.
[12] Halder A, Choudhury D, Ghosh S, Subbiah AS, Sarkar SK. Exploring thermochromic behavior of hydrated hybrid perovskites in solar cells. J Phys Chem Lett 2015;6(16):3180–4.
[13] Zhang Y, Tso C, Iñigo JS, Liu S, Miyazaki H, Chao CY, Yu KM. Perovskite thermochromic smart window: advanced optical properties and low transition temperature. Appl Energy 2019;254:113690.
[14] Liu S, Du YW, Tso CY, Lee HH, Cheng R, Feng S-P, Yu KM. Organic hybrid perovskite (MAPbI 3−xClx) for thermochromic smart window with strong optical regulation ability, low transition temperature, and narrow hysteresis width. Adv Funct Mater 2021;31(26):2010426.
[15] Rosales BA, Mundt LE, Allen TG, Moore DT, Prince KJ, Wolden CA, Rumbles G, Schelhas LT, Wheeler LM. Reversible multicolor chromism in layered formamidinium metal halide perovskites. Nat Commun 2020;11(1):5234.
[16] Suichi T, Ishikawa A, Hayashi Y, Tsuruta K. Performance limit of daytime radiative cooling in warm humid environment. AIP Adv 2018;8(5):055124.
[17] Raman AP, Abou Anoma M, Zhu L, Rephaeli E, Fan S. Passive radiative cooling below ambient air temperature under direct sunlight. Nature 2014;515(7528):540–4.
[18] Jeong SY, Tso CY, Ha J, Wong YM, Chao CY, Huang B, Qiu H. Field investigation of a photonic multi-layered TiO2 passive radiative cooler in sub-tropical climate. Renew Energy 2020;146:44–55.
[19] Hervé A, Drevillon J, Ezzahri Y, Joulain K. Radiative cooling by tailoring surfaces with microstructures: association of a grating and a multi-layer structure. J Quant Spectrosc Radiat Transf 2018;221:155–63.
[20] Zhu L, Raman AP, Fan S. Radiative cooling of solar absorbers using a visibly transparent photonic crystal thermal blackbody. Proc Natl Acad Sci Unit States Am 2015;112(40):12282–7.
[21] Zou C, Ren G, Hossain MM, Nirantar S, Withayachumnankul W, Ahmed T, Bhaskaran M, Sriram S, Gu M, Fumeaux C. Metal-loaded dielectric resonator metasurfaces for radiative cooling. Adv Opt Mater 2017;5(20):1700460.
[22] Rephaeli E, Raman A, Fan S. Ultrabroadband photonic structures to achieve high-performance daytime radiative cooling. Nano Lett 2013;13(4):1457–61.
[23] Hossain MM, Jia B, Gu M. A metamaterial emitter for highly efficient radiative cooling. Adv Opt Mater 2015;3(8):1047–51.
[24] Jia Z-X, Shuai Y, Li M, Guo Y, Tan H-p. Enhancement radiative cooling performance of nanoparticle crystal via oxidation. J Quant Spectrosc Radiat Transf 2018;207:23–31.
[25] Wu D, Liu C, Xu Z, Liu Y, Yu Z, Yu L, Chen L, Li R, Ma R, Ye H. The design of ultra-broadband selective near-perfect absorber based on photonic structures to achieve near-ideal daytime radiative cooling. Mater Des 2018;139:104–11.
[26] Jeong S, Tso CY, Wong YM, Chao CY, Huang B. Daytime passive radiative cooling by ultra emissive bio-inspired polymeric surface. Sol Energy Mater Sol Cell 2020;206:110296.
[27] Kou J-l, Jurado Z, Chen Z, Fan S, Minnich AJ. Daytime radiative cooling using near-black infrared emitters. ACS Photonics 2017;4(3):626–30.
[28] Marino C, Minichiello F, Bahnfleth W. The influence of surface finishes on the energy demand of HVAC systems for existing buildings. Energy Build 2015;95:70–9.
[29] Gao Y, Xu J, Yang S, Tang X, Zhou Q, Ge J, Xu T, Levinson R. Cool roofs in China: policy review, building simulations, and proof-of-concept experiments. Energy Pol 2014;74:190–214.
[30] Saeli M, Piccirillo C, Parkin IP, Binions R, Ridley I. Energy modelling studies of thermochromic glazing. Energy Build 2010;42(10):1666–73.
[31] Hoffmann S, Lee ES, Clavero C. Examination of the technical potential of near-infrared switching thermochromic windows for commercial building applications. Sol Energy Mater Sol Cell 2014;123:65–80.
[32] Ye H, Meng X, Xu B. Theoretical discussions of perfect window, ideal near infrared solar spectrum regulating window and current thermochromic window. Energy Build 2012;49:164–72.
[33] Li T, Zhai Y, He S, Gan W, Wei Z, Heidarinejad M, Dalgo D, Mi R, Zhao X, Song J. A radiative cooling structural material. Science 2019;364(6442):760–3.
[34] Beck HE, Zimmermann NE, McVicar TR, Vergopolan N, Berg A, Wood EF. Present and future Köppen-Geiger climate classification maps at 1-km resolution. Scientific Data 2018;5:180214.
[35] Office of Energy Efficiency and Renewable Energy, The U.S. Department of Energy. Commercial reference buildings. https://www.energy.gov/eere/buildings/commercial-reference-buildings. [Accessed 5 May 2020].
[36] Allen E, Iano J. Fundamentals of building construction: materials and methods. John Wiley & Sons; 2019.
[37] Lawrence Berkeley National Laboratory. Building technology and urban systems. July. 3, 2019. WINDOW 7.7, https://windows.lbl.gov/software/window. [Accessed 5 May 2020].
[38] EnergyPlus. EnergyPlus Documentation, input Output reference. Sep. 29, 2020. https://energyplus.net/documentation. [Accessed 5 May 2020].
[39] Los Alamos National Laboratory (LANL). Sustainable design guide, chapter 4: the building architectural design. https://www.energy.gov/eere/buildings/advanced-energy-design-guides. [Accessed 3 November 2020].